WHITE PAPER

Inductive SMT Components in Comparison – the Wire Makes the Difference

Dr.-Ing. (Doctor of Engineering) Heinz Zenkner

1. INTRODUCTION

This white paper concisely shows the differences between three different inductive SMT components – the ceramic inductor (air coil), the SMT ferrite and the wire-wound ferrite inductor. Electrical parameters are compared and their differences explained. Applications to illustrate how the components can be used to the best performance and how physically induced parasitic parameters can be used advantageously in circuit design.

2. COMPARISON OF THE SMT FERRITE, CERAMIC/AIR INDUCTOR AND WIRE-WOUND FERRITE

Figure 1 shows the impedance curves of the three inductor types:

- WE - CBF: SMT ferrite
- WE - KI: SMT inductor with ceramic core ('air coil')
- WE - RFI: Wire windings on a ferrite core ('wire-wound ferrite')

The components were selected such that, below their respective maximum impedance, they have a similar impedance curve. The differences in impedances are significant in the frequency region at which the maximum is achieved.

The SMT ferrite attains its maximum at the lowest frequency, while the wire-wound ferrite attains its maximum at the highest frequency. The ceramic inductor has the steepest rise and fall around the impedance maximum and therefore the highest Q factor and narrower bandwidth.

2.1 Comparison of electrical parameters

Figure 2 compares the electrical parameters of the inductors.

For inductors without a ferrite core (WE - KI), the inductance is specified as a value in data sheets, in this case 560 nH. Although the inductance value is a function of the measuring frequency, below the resonant frequency the value is almost constant against frequency (see data sheet).

Taking a closer look, the reactance of the inductor does not increase linearly with frequency. There are two effects that raise the impedance of the air coil: The increase in reactance described by Lenz's law and the increase in resistance from the skin effect.

In the purely inductive circuit, the coil is connected directly to the AC supply voltage. As the voltage rises and falls with frequency, the self-induced counter-electromotive force (counter EMF) in the coil also rises and falls dependent on this change.

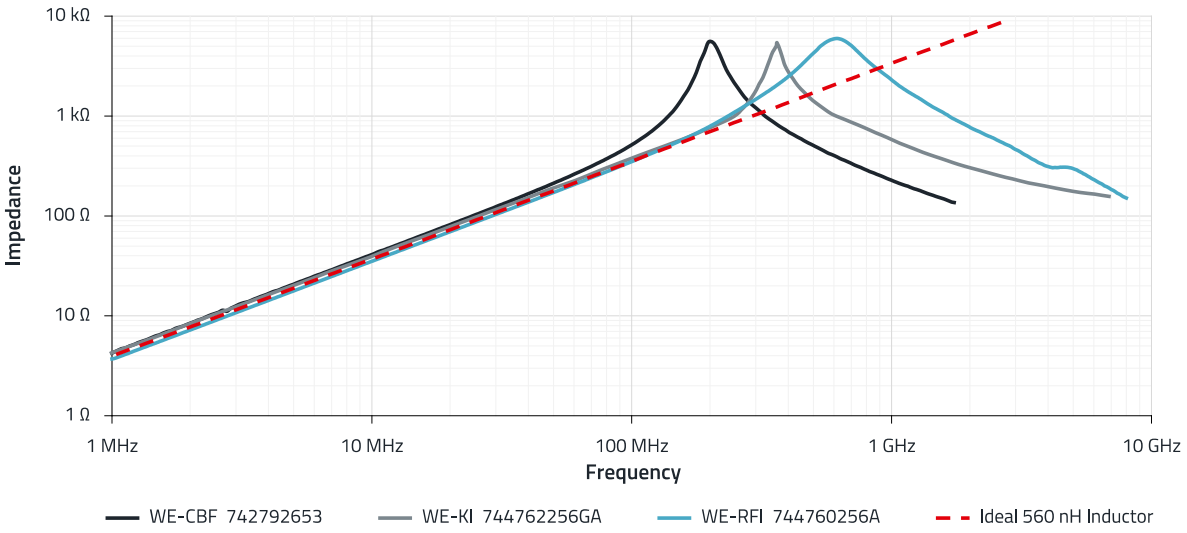

Figure 1: Comparison of SMT ferrite, ceramic/air inductor and wire-wound ferrite.

WE-KI ceramic SMT inductor 744762256GA

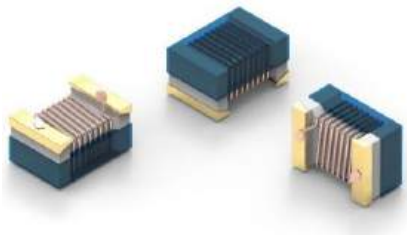

Properties		Test conditions	Value	Unit	Tol.
Inductance	L	25 MHz	560	nH	±2%
Q-Factor	Q	100 MHz	45		min.
DC Resistance	R_{DC}	@ 20 °C	1.5	Ω	max.
Rated Current	I_R	ΔT = 15 K	310	mA	max.
Self Resonant Frequency	f_{res}		430	MHz	min.

WE-CBF SMT ferrite 742792653

Properties		Test conditions	Value	Unit	Tol.
Impedance @ 100 MHz	Z	100 MHz	600	Ω	±25%
Maximum Impedance	Z_{max}	200 MHz	4500	Ω	typ.
Rated Current 1	I_{R1}	ΔT = 20 K	300	mA	max.
Rated Current 2	I_{R2}	ΔT = 40 K	500	mA	max.
DC Resistance	R_{DC}	@ 20 °C	0.65	Ω	max.
Type	High Speed				

WE-RFI ferrite SMT inductor 744760256A

Properties		Test conditions	Value	Unit	Tol.
Inductance	L	25.2 MHz	0.56	µH	±5%
Q-Factor	Q	100 MHz	45		min.
Impedance @ 100 MHz	Z	100 MHz	350	Ω	±25%
Maximum Impedance	Z_{max}	600 MHz	5570	Ω	typ.
Rated Current 1	I_{R1}	ΔT = 15 K	450	mA	max.
Rated Current 2	I_{R2}	ΔT = 40 K	620	mA	max.
DC Resistance	R_{DC}	@ 20 °C	0.55	Ω	max.
Self Resonant Frequency	f_{res}		340	MHz	min.

Figure 2: Comparison of parameters according to Figure 1.

It is known that this self-induced counter-EMF is directly proportional to the rate of change of the current through the coil (Lenz's law) and therefore increases with frequency. This means that the reactance of the inductor also increases with frequency; this relationship is proportional.

A further increase in impedance comes from the skin effect. At low frequencies, a conductor uses almost its entire cross-sectional area as a medium to transport charge carriers. If the frequency is increased, an increased magnetic field along the center of the conductor represents an impedance for the charge carriers, which causes the current density in the center of the conductor to decrease and the current density around the edge of the conductor to increase. This increased current density near the edge of the conductor is known as the skin effect. The effect increases with frequency and also occurs in all other inductors (with ferrite core).

Without a ferrite core, the resonant frequency of the inductor is primarily caused by the parasitic capacitance between the individual winding. Whenever two conductors are in close proximity, but separated by a dielectric material, and there is a voltage difference between them, a capacitor is formed.

The chain of these winding capacitances is connected in parallel with the winding inductance thus forming a parallel resonant circuit. There is also a parasitic capacitance between the connectors (solder pads) in parallel with the winding capacitance. The resulting equivalent circuit is a parasitic total capacitance in parallel with the winding. The equivalent circuit in this case is shown in Figure 3 on the left.

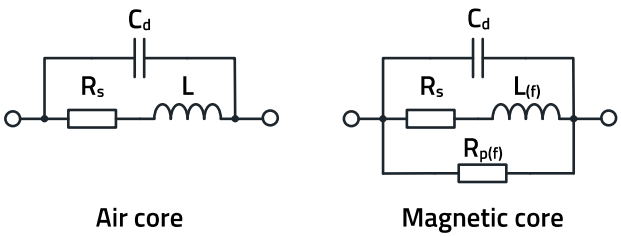

Figure 3: Equivalent circuit for an inductor without magnetic core (left) and with magnetic core (right).

In case of inductors with a ferrite core (WE - RFI) and SMT ferrites (WE - CBF), the data sheet does not specify an inductance value, but rather the impedance at a measuring frequency.

It is also apparent that the SMT ferrite has the highest tolerance, while the inductor without ferrite has the lowest tolerance.

As the WE - KI inductor does not have a ferrite core, it requires more turns of wire for the same impedance than components with ferrite. This is why the WE - KI has the highest wire resistance R_{DC} for the same inductance. A Q-factor (quality factor) is specified for both the WE - KI and the WE - RFI, but not for the WE - CBF. The Q-factor (Q) is a measure of the dissipative property of an inductor. Inductors with a high Q-factor have lower losses and a narrower-band impedance curve. Chokes with a low Q-factor, however, have higher losses and a broader-band impedance curve. The level of the maximum impedance of the inductor is related to the quality factor Q. Low-loss inductors with a high Q-factor have a very high maximum impedance, while inductors with high loss have a lower maximum impedance. Changing the way a coil is wound or the core materials used can align the maximum impedance and the frequency range of that impedance maximum. What role does the impedance maximum play?

3. MAGNETIC CORE MATERIALS

Figure 4 shows the impedance curves against frequency for the WE - RFI inductor and WE - CBF SMT ferrite. Both components have ferrites as their core material. The graphs show three different curves respectively, R – as resistive (ohmic) resistance, X_L – as reactance (inductive) and Z – as the component's impedance. In order to be able to successfully use inductors with ferrite material, it is important to understand these graphs.

In many high-frequency applications in which high inductance values are required in a small space, 'air core' inductors cannot be used on account of their size.

The package of the inductor becomes smaller if the air core is replaced by a core material with higher magnetic permeability ($\mu_r > 1$).

For components of the same size but with a ferrite core, the same inductance value is achieved at a certain frequency with a smaller number of turns.This can carry out several advantages.

- Smaller size – from the lower number of turns required for a certain inductance.
- Increased quality Q – fewer windings mean lower wire resistance.
- Influencing the impedance of the inductance against frequency – through specific selection/mixing of the core material.

However, the use of magnetic cores presents some big problems and attention must be paid to ensure that the core material chosen is the right one for the job. Some of these problems:

- Every core material is highly lossy above a certain frequency range. Adding a magnetic core to an air-core coil for example can reduce the quality Q of the inductor, depending on the material used and the operating frequency.
- The permeability of all magnetic cores changes with frequency and usually drops to a very low value at the upper end of the operating range. It eventually approaches the permeability of air ($\mu_r = 1$) and becomes 'invisible' for the circuit.
- The higher the permeability of the core, the more sensitive it is to temperature fluctuations.

  So the inductance of the coil can fluctuate considerably across a broad temperature range.

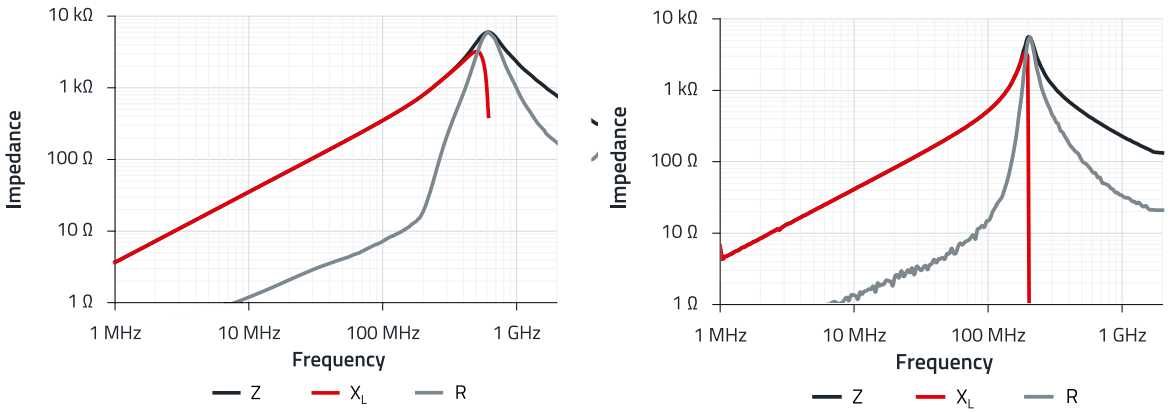

RFI - 744760256A

CBF - 742792653

Figure 4: Typical impedance curves for the WE - RFI inductor and the WE - CBF SMT ferrite.

- The permeability of the magnetic core changes with the applied signal level. If there is excessive current through the inductor and the magnetic flux density through the core becomes too high, this leads to saturation of the core.

These problems can be overcome if care is taken during development to ensure that the inductors are selected correctly according to their application and this requires the impedance graphs with the three different impedance curves R, X_L and Z. The progression of the curves against frequency depends strongly on the magnetic properties of the core material.

The equivalent circuit of an inductor without a magnetic core is shown in Figure 3 on the left.

The Q value of this inductor with 'air core' is

$$Q = \frac{X_L}{R_S} \quad (1)$$

where

$$X_L = \omega \cdot L \quad (2)$$

R_S is the resistance of the winding.

If we add a magnetic core to the inductor, the result is the equivalent circuit shown in Figure 3 on the right. We added the resistance $R_{p(f)}$ to represent the losses occurring in the core itself. These frequency-dependent losses occur in the form of magnetic hysteresis. Hysteresis is power loss in the core that occurs due to eddy currents and by energy consumed during realignment of the magnetic particles in the material with change in magnetization. Eddy currents flow in the core caused by the currents induced in it. We also assigned frequency dependence $L_{(f)}$ to the inductor L, since, as previously mentioned, the magnetic permeability of the material is non-linear against frequency f. The quality Q of an inductor with ferrite core is therefore a variable parameter that depends on the current flowing through the inductor and its frequency, and hence has to be determined individually.

Ferrite is a material that mainly contains iron. It is manufactured from a mixture of iron oxide and other trace metal oxides. As the material has low electrical conductivity, it keeps eddy currents and their associated losses low. A special property of these materials is their strong dependence on frequency, magnetic flux density and temperature.

3.1 Complex permeability

The magnetic property of materials can be described by their 'magnetic permeability' μ. Permeability μ describes a property that quantifies the magnetic response of the flux density B when the material is exposed to a magnetic field strength H. The magnetic permeability is proportional to the ratio of the changes in B and H:

$$\mu = \frac{\Delta B}{\Delta H} \quad (3)$$

The value of the absolute permeability μ expresses the direct ratio of B (T) to H (A / m), so the resulting SI unit is (H / m). The relative permeability has no units and relates to the permeability of vacuum (μ_0) and is usually specified in inductor data sheets. The relative values are an easily comprehensible indicator that describes the extent to which the material 'concentrates' the magnetic field 'better' than a vacuum.

This results in the following relationship

$$\mu = \mu_r \cdot \mu_0 \quad (4)$$

with μ_0: magnetic permeability of vacuum:
1.26×10^{-6} (H / m).

Most of the ferrite materials used are iron oxide mixtures with manganese-zinc (MnZn) and nickel-zinc (NiZn); μ_r is typically in the range of 600 to 15,000 for MnZn and 10 to 1,500 for NiZn. It should be noted that the relative permeability depends strongly on the frequency of the magnetic field. Furthermore, the curves in Figure 4 already indicate that the relative magnetic permeability has two parts, a real part μ_r' and an imaginary part μ_r''. This complex permeability takes effect with high-frequency magnetic field interaction in which a phase shift occurs between H and B.

This results in:

$$\mu = \frac{B_0 \cdot e^{j(\omega t-\delta)}}{H_0 \cdot e^{j\omega t}} = \frac{B_0}{H_0} \cdot e^{-\delta} = \frac{B_0}{H_0} \cdot \cos(\delta) - j \cdot \frac{B_0}{H_0} \cdot \sin(\delta) \quad (5)$$

If we apply the above result to the inductance with ferrite core, we obtain two important formulas for the series equivalent circuit:

$$L_S = \mu' \cdot L_0 \quad (6)$$

$$R_S = \mu'' \cdot \omega \cdot L_0 \quad (7)$$

where L_0 is the inductance of the wire winding without ferrite.

The following relationship applies:

$$\underline{Z} = j \cdot \omega \cdot L_0 \cdot (\mu' - j \cdot \mu'') = R + j \cdot X \qquad (8)$$

L_0: inductor without ferrite.

It is easy to see from the formulas that high permeability leads to high inductance, but high permeability is usually associated with higher core losses at high frequencies.

The individual components of the impedance, i.e., $Z_{(f)}$, $X_{L(f)}$ and $R_{(f)}$, are depicted in the data sheets for ferrite inductors. Figure 5 now shows again the impedance curves for the WE - RFI inductor 744760256A.

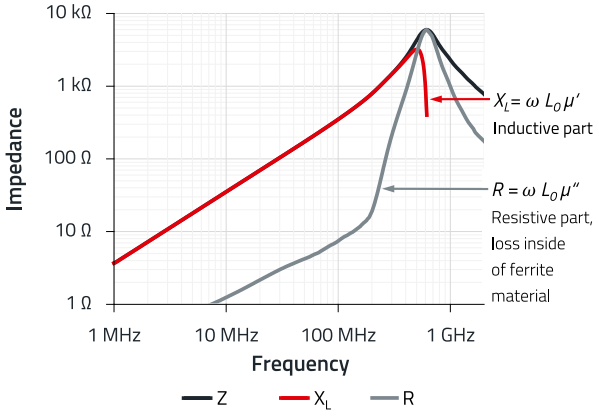

Figure 5: Impedance curves of the WE - RFI inductor 744760256A.

This also makes it clear why the impedance curves are of such importance for a functioning circuit using inductors with a ferrite core. The impedance (Z) is a vector combination of resistance and phase. The ohmic resistance R has a dissipative property, energy is consumed and not returned. The reactance X_L is the part of the impedance generated by inductance. The phase is the delay between a voltage applied to the component and the current flowing through it. Both the resistive losses and the reactance vary with frequency, and therefore also with phase.

But that's not all. Magnetic materials show saturation effects against frequency, primarily depend on the magnetic flux density, i.e., the current flowing through the ferrite inductor. This is referred to as core saturation, an effect that 'air inductors' do not have. Figure 6 shows the impedance of the two inductors WE - RFI 744760256A and WE - CBF 742792653 having different DC bias magnetization (DC bias) against frequency. The difference is clearly apparent.

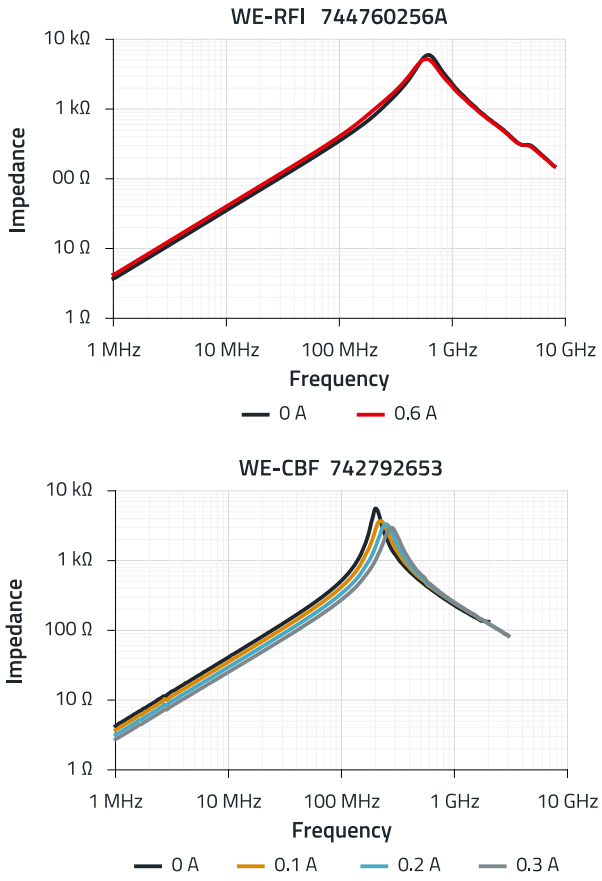

Figure 6: Impedance of the two inductors WE - RFI 744760256A and WE - CBF 742792653 having different DC bias magnetization against frequency.

Wire-wound inductors are less sensitive to DC pre-saturation (current bias) than SMT ferrites for the same rated current.

The influence of bias magnetization of different levels on the impedance curves can be simulated with the help of Redexpert for all article numbers.

How is it with 'HF performance'? Figure 7 shows the electrical performance of WE - RFI 744762415A.

What is the meaning of the different impedance performance curves according to Figure 7? To illustrate the impedance behavior of the inductor, a setup described by Tektronix[1] was selected. Figure 8 shows a photo of the measuring adapter in the lab setup.

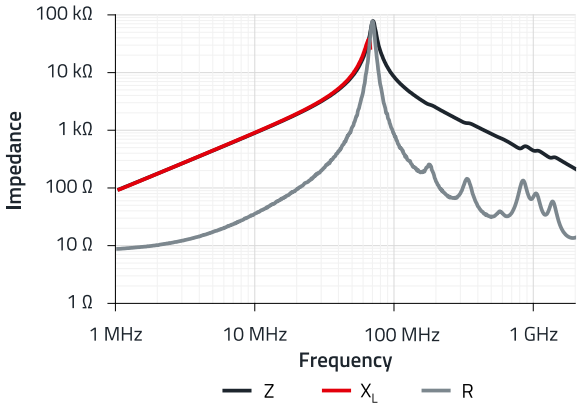

Figure 7: Typical impedance curve of an 'RFI inductor'.

The measurement results are shown in Figure 9. The three images below show the oscillograms of the voltages U_a (yellow) and U_b (blue) in phase relation to each other at three typical measuring frequencies. In the left image, the component (inductor) behaves inductively, the phase angle is positive, in the middle image the phase offset is 0°, i.e., the component is resistive, and in the right image the phase offset is negative; here the component behaves capacitively.

3.2 Simple impedance measurement method

The curve on the left in the lower section of Figure 9 shows the voltage U_b against frequency. The voltage is a relative measure for the magnitude of impedance of the component or inductor. The curve on the right shows the phase offset between voltage U_b and voltage U_a and thus the 'behavior' of the component under test. Up to a frequency of 26 MHz, the component behaves inductively, the phase progression is positive and extends from approx. 85° to 0°, i.e., the inductive impedance part falls

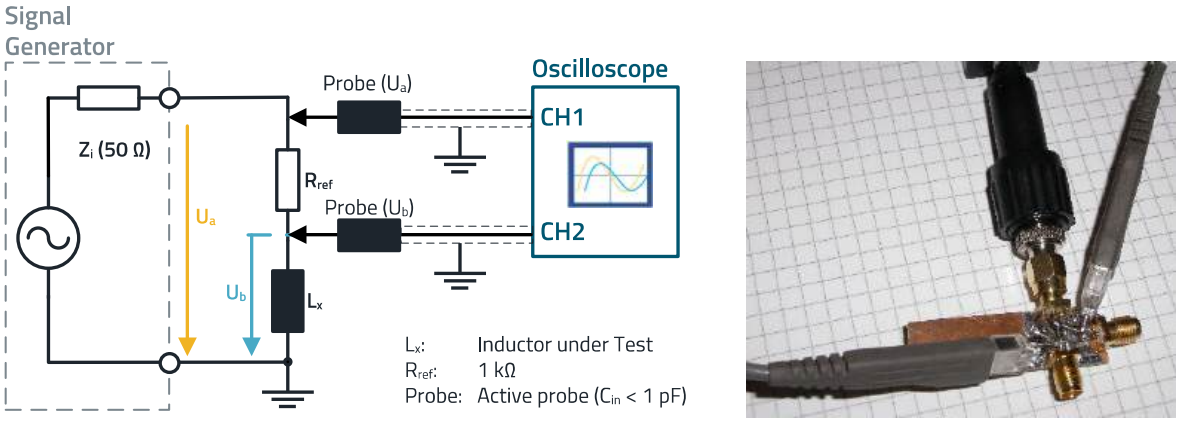

Figure 8: Left: schematic setup for measuring the phase progression of the inductors; Right: Lab setup of the measuring adapter.

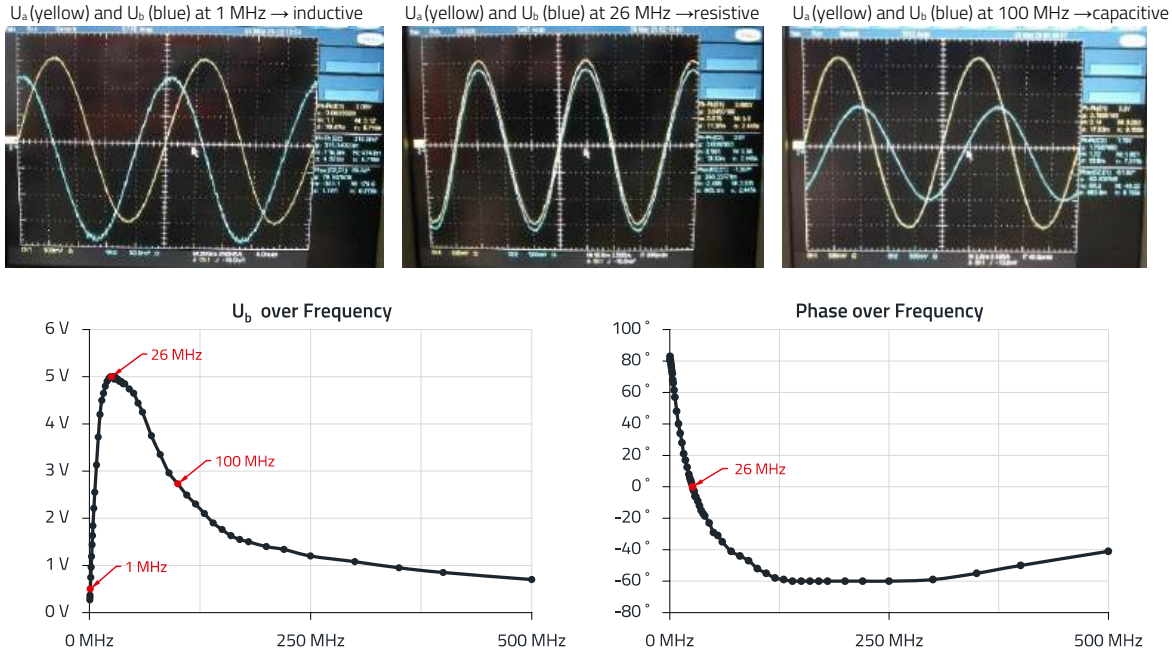

Figure 9: Measurement results for the two voltages U_a and U_b for WE - RFI 744762415A according to Figure 8.

and the resistive impedance part rises due to the ferrite material. At 0°, the inductor reaches its resonant frequency of 26 MHz. Here is the maximum (curve on the left). Above 26 MHz the impedance falls off sharply. The component is capacitive, with a resistive impedance part of it from the ferrite material.

The phase, from 0° at 26 MHz drops to - 60° and then rises with increasing frequency to - 40° at 500 MHz.

This also makes sense of the impedance curves shown in the data sheets. These are the magnitudes of the impedances. In Figure 7 this means: The black curve represents the impedance, which, analogous to our measurement, corresponds to the magnitude of U_b. The red curve is the impedance at which the phase is positive, i.e., here the component predominantly behaves inductively in the lower frequency range until the resistive impedance part steadily increases. In the range of the highest impedance, i.e., the resonance range, the gray curve, which corresponds to the resistive ('ohmic') part of the impedance, has its maximum. The resistive part is only found in inductors with a ferrite core and represents the losses of the ferrite material against frequency.

4. PREFERRED APPLICATIONS FOR THE INDUCTORS

The properties of the inductors described above explain why each type of component has its own preferred applications. The clearest way to demonstrate this is with specific application examples, and so a complete circuit for generating reference signals is presented below. Figure 10 shows the block diagram for the signal generator. The inductive filter components subject to the following measurements of interference levels are also shown.

4.1 Signal section

A 20 MHz quartz oscillator generates a square-wave signal that is divided into three square-wave signals of different frequencies through frequency dividers:

- 100 kHz, duty cycle (DC): 40%
- 1 MHz, duty cycle (DC): 20%
- 5 MHz, duty cycle (DC): 50%

The 1 MHz signal (DC: 20%) is converted to a 50% duty cycle with the positive edge of a monoflop. The monoflop is followed by a fifth-order low-pass filter with a cut-off frequency of 1.1 MHz, which effectively attenuates the harmonics of the square-wave signal.

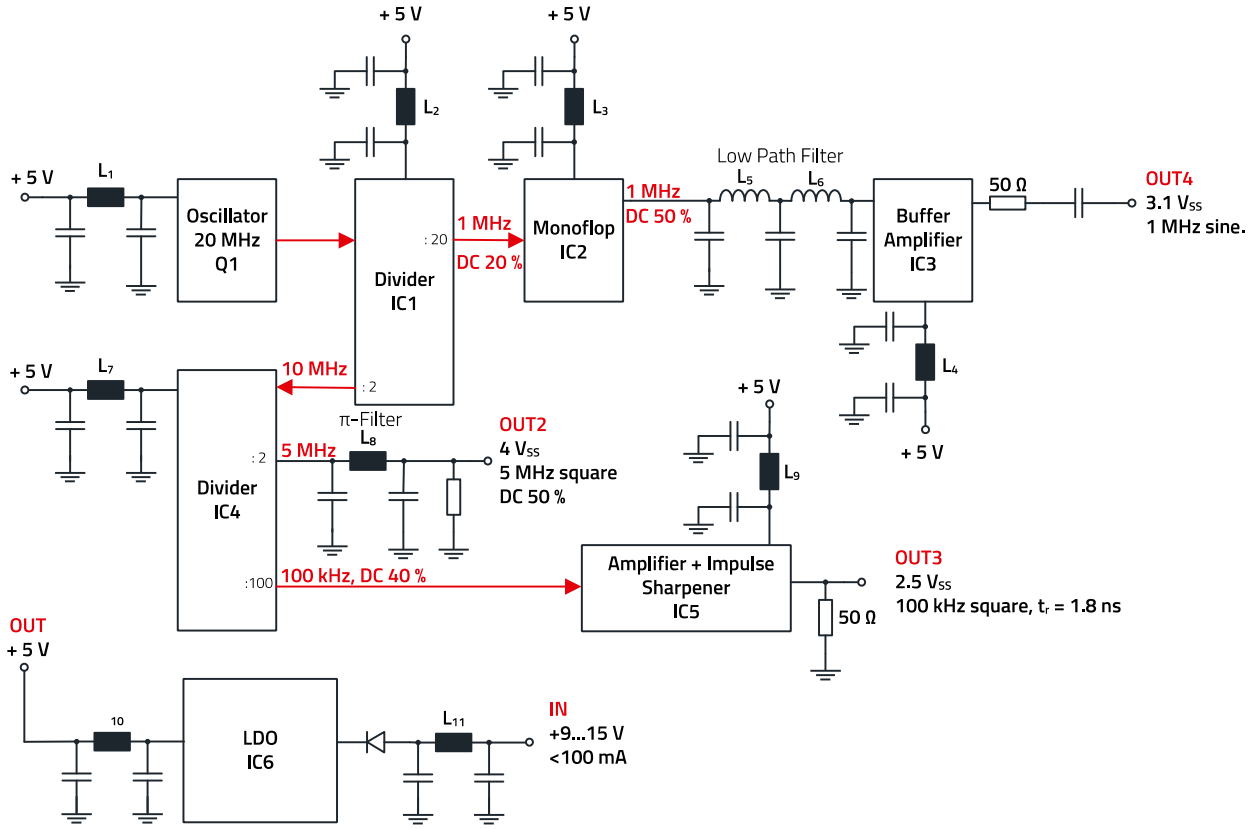

Figure 10: Block diagram of the signal generator.

A low-noise operational amplifier buffers the signal, which is then available at output 4 with 3.1 V_{ss} at 50 Ω.

Harmonics, interference spectrum

The spectrum of the 1 MHz sine-wave output signal is shown in Figure 11.

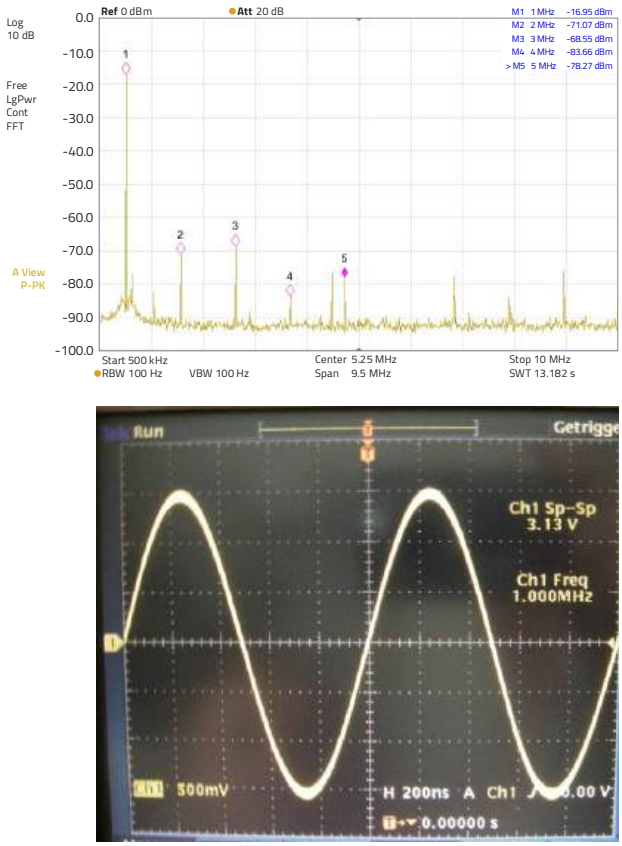

Figure 11: 1 MHz sinus signal at output 4. Above: in the frequency domain; Below: in the time domain.

The second harmonic of the signal is 54 dB, the third is 52 dB and the fourth 67 dB below the signal level; the fifth-order filter and a low-distortion operational amplifier are at the output. The filter (L_5, L_6 with C_6, C_7 and C_8 from the circuit diagram in Figure 13) is set up with WE - RFI wire-wound ferrite inductors 744760410A and MLCC capacitors. The 10 µH inductor has its resonant frequency at 40 MHz, so mainly the inductive range of the component's impedance is used in this application. Although the resistive part of the impedance reduces the quality Q of the filter, it also effectively attenuates possible resonances, so a high overall insertion loss is achieved.

Signal matching, signal filtering

The 5 MHz square-wave signal is 'freed' of high-frequency harmonics by the output filter with L_8 and C_{13}, C_{14}. The signal relationships in the time and frequency domain are shown in Figure 12.

The π-filter is set up with a WE - CBF SMT ferrite 742792653. The rise and fall times are slowed down by the filter from approx. 7 ns to 13 ns. In the frequency domain (lower image in Figure 12) it is clear that above approx. 20 MHz the filter has an attenuation of 10 dB.

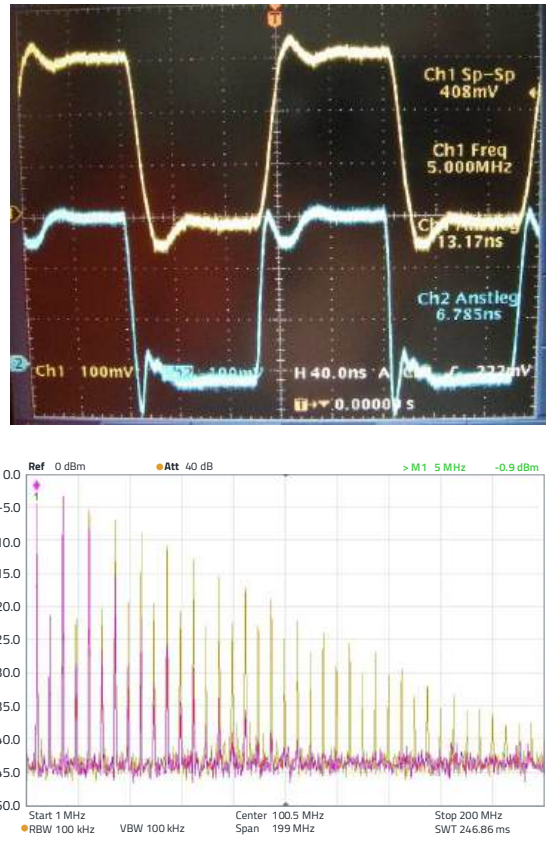

Figure 12: 5 MHz square-wave signal at output 2. Above in the time domain: 10 : 1 divider, blue: Before filter, yellow: After filter. Below: Measurement in the frequency domain with HF probe.

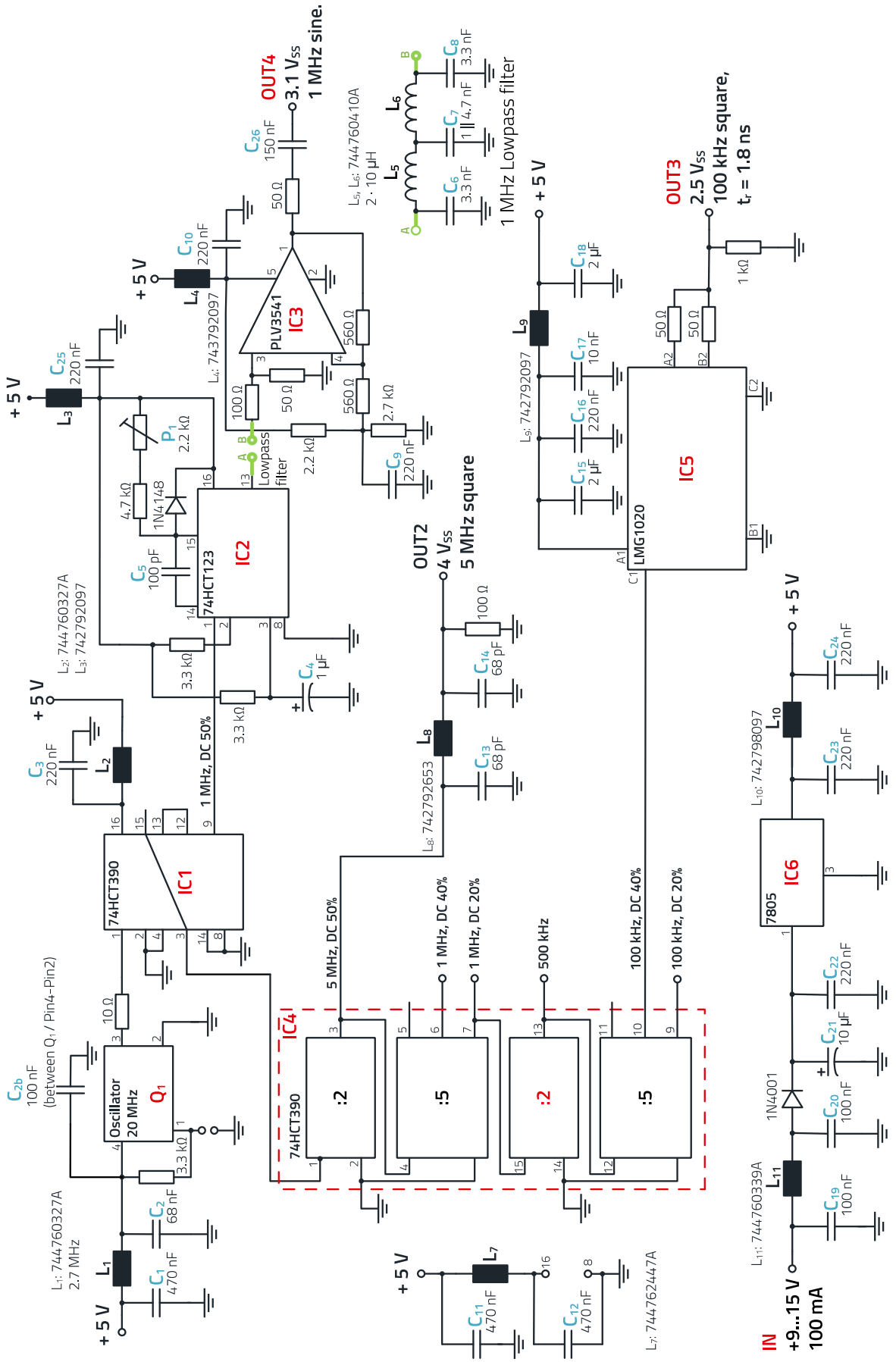

Figure 13: Circuit diagram of the signal generator.

Of course, the cut-off frequency can be shifted up by using smaller capacitance values for C_{13} and C_{14}, which shortens the rise and fall times. The resistive component of the SMT ferrite attenuates the harmonics in this filter. In the range above 80 MHz, the resistive component of the ferrite's impedance rises sharply (data sheet), such that no overshoots and resonances can occur through the 'pulsating' square-wave signal.

The 100 kHz square-wave signal at output 3 (Figure 10) has a level of 2.5 V_{ss}, a DC of 40%, an output impedance of 50 Ω and a signal rise time t_r of < 2 ns.

The signal decay time t_f is < 4 ns. Figure 14 shows the signal.

The signal is divided from 10 MHz to 100 kHz by the 100 : 1 divider (Figure 10) and then goes to the output driver. The component LMG1020 (Texas Instruments) is a 'low-side ultra-fast gate driver' and with a suitably adapted layout, the rise and fall times can be further reduced to below 1 ns.

The entire circuit diagram is shown in Figure 13. The signal source and the three signal paths are apparent, analogous to the block diagram in Figure 10.

- 20 MHz quartz oscillator Q1, WE-SPXO 830201878701
- Frequency divider IC1, 20:1 (1 MHz) → monoflop IC2 → 5th order filter → output buffer IC 3 → output 1 MHz sine-wave signal.
- Frequency divider IC1, 2:1 (10 MHz) → Frequency divider IC4a, 2 : 1 (5 MHz) → 3rd order filter → output 5 MHz square wave signal.
- Frequency divider IC4b, 10:1 (1 MHz from IC4a to 100 kHz) → gate driver IC5 → output 100 kHz square wave signal with short rising edge.

A linear regulator (IC6) with steep input and output filters, which are explained in the next section 4.2. The current consumption of the entire circuit is less than 100 mA at 9 V.

Pulse period, 2.5 V_{ss}, 100 kHz, duty cycle 40%

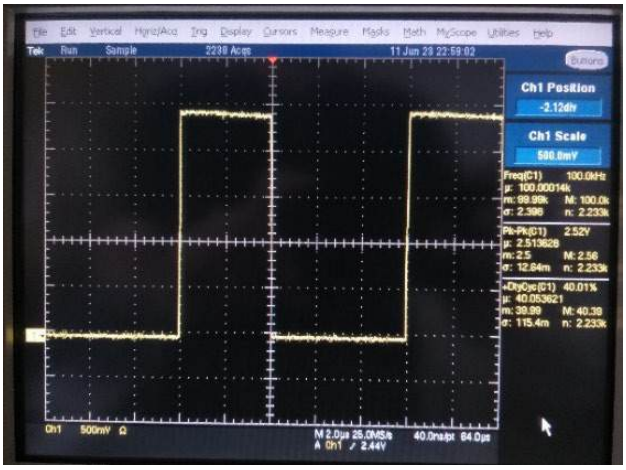

Rise time 1.65 ns

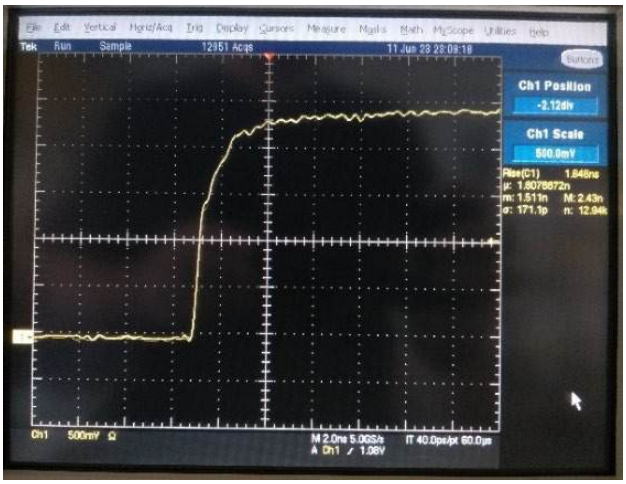

Fall time 3.83 ns

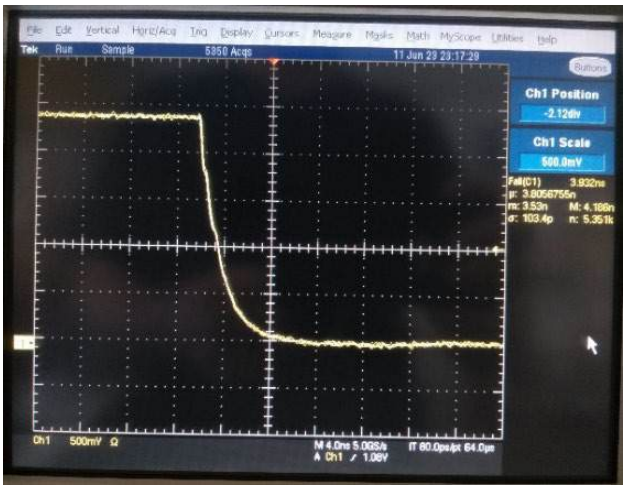

All measurements at the 50 Ω input:

Figure 14: 100 kHz signal at output 3, measured at the 50 Ω oscilloscope input.

4.2 Decoupling the power supply at the ICs

The measures for supplying power to the ICs with the relevant filters to reduce local emissions are shown as follows. A π-filter can generally be assumed, as can be seen from Figure 10. The reason is that

- each IC requires a decoupling capacitor directly at the IC in order to keep the differential mode interference loop alongside the IC small and to provide a bypass capacitor for the transient charging currents during the switching process of the IC.
- bypass capacitors are also provided on the primary side of the inductor, i.e., at the input of the filter on the power supply side.

This filter topology is illustrated in Figure 15.

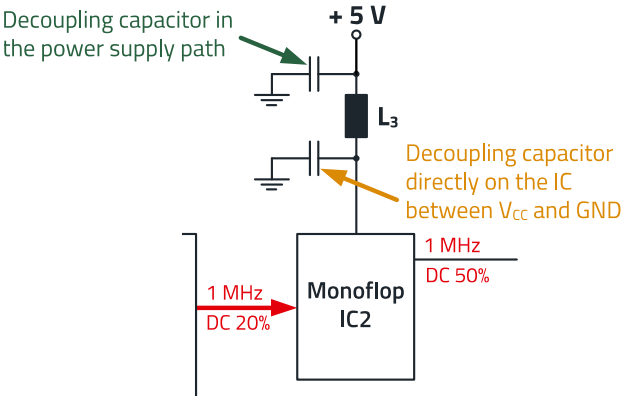

Figure 15: π-filter topology for attenuating the interference emission from the ICs.

To show the filter efficiency and the associated inductive components selected, a spectrum analyzer was used to record the frequency spectrum before and after the filter, i.e., over the bandwidth of interest in each case. The graphs are assigned as shown in Figure 18.

The individual measurement results:

PNG1:

The power supply to the quartz oscillator is decoupled by a WE - RFI inductor 744760327A, Figure 16 shows the emission spectrum before and after the choke.

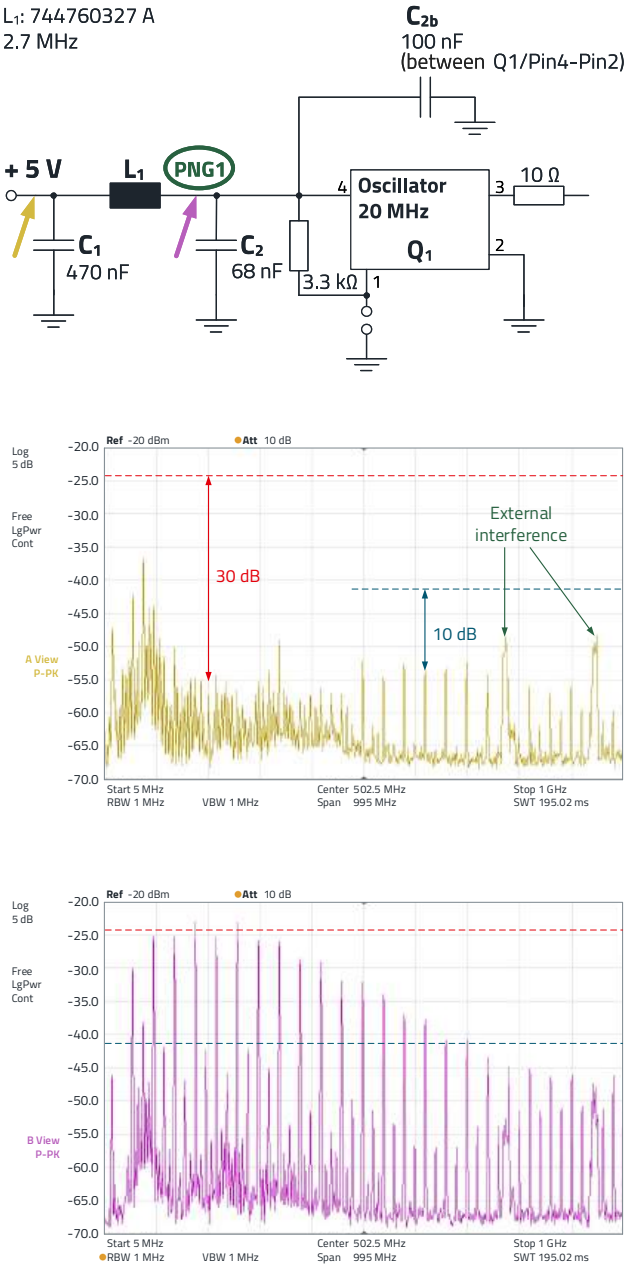

Figure 16: PNG1: 20 MHz oscillator – V_{cc} – decoupling. Yellow: after the choke. Purple: before the choke.

The choke has an inductance of 2.7 µH, but a high impedance of over 1.5 kΩ in the frequency range above approx. 100 MHz as a result of the ferrite core. The reduction of the emission spectrum is up to 30 dB in the range from 100 to 400 MHz, above 400 MHz the attenuation falls to 25 dB and drops to approx. 10 dB up to 1 GHz.

PNG2:

The frequency divider IC1 divides the 20 MHz signal by 20 reducing it to 1 MHz. 74HCT390 is a dual 4-bit decade ripple counter that is divided into four separate function blocks. The counters have two function blocks that divide by 2 and another two that divide by 5. As two separate counters are installed in one IC housing, frequency division applications with division by 2, 4, 5, 10, 20, 25, 50 or 100 are possible.

The serial, asynchronous functionality results in different duty cycles (DC) and thus also narrow-band interference spectra distributed over a wide frequency range. The circuit diagram extract with the associated interference spectra is shown in Figure 17.

The WE - RFI inductor 744760327A is also used here. The reduction of the interference spectrum is approx. 22 dB in the 100 MHz frequency range and decreases to approx. 10 dB at 1 GHz.

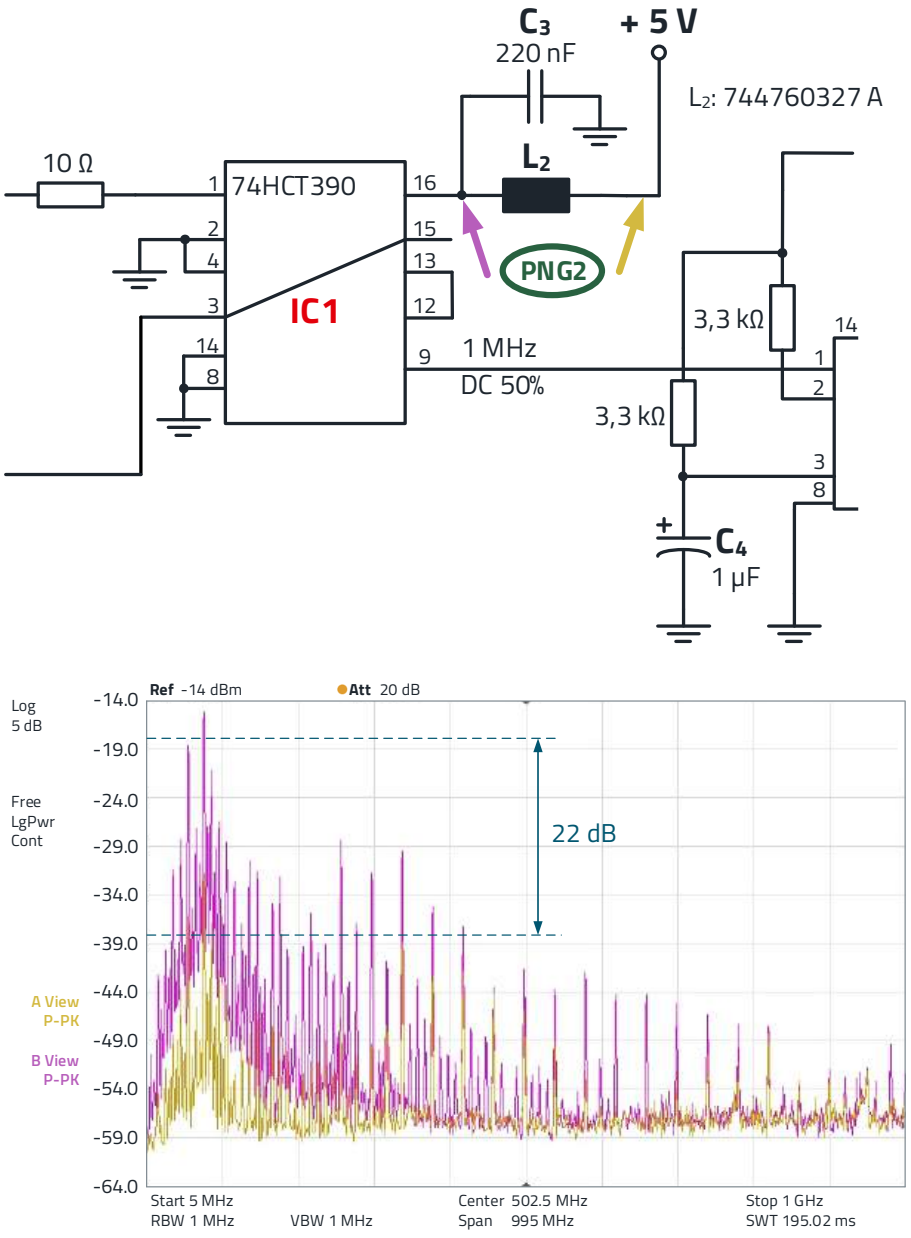

Figure 17: PNG2: V_{cc} – Decoupling at frequency divider IC1 with the associated interference spectra. Purple: before the choke, Yellow: after the choke.

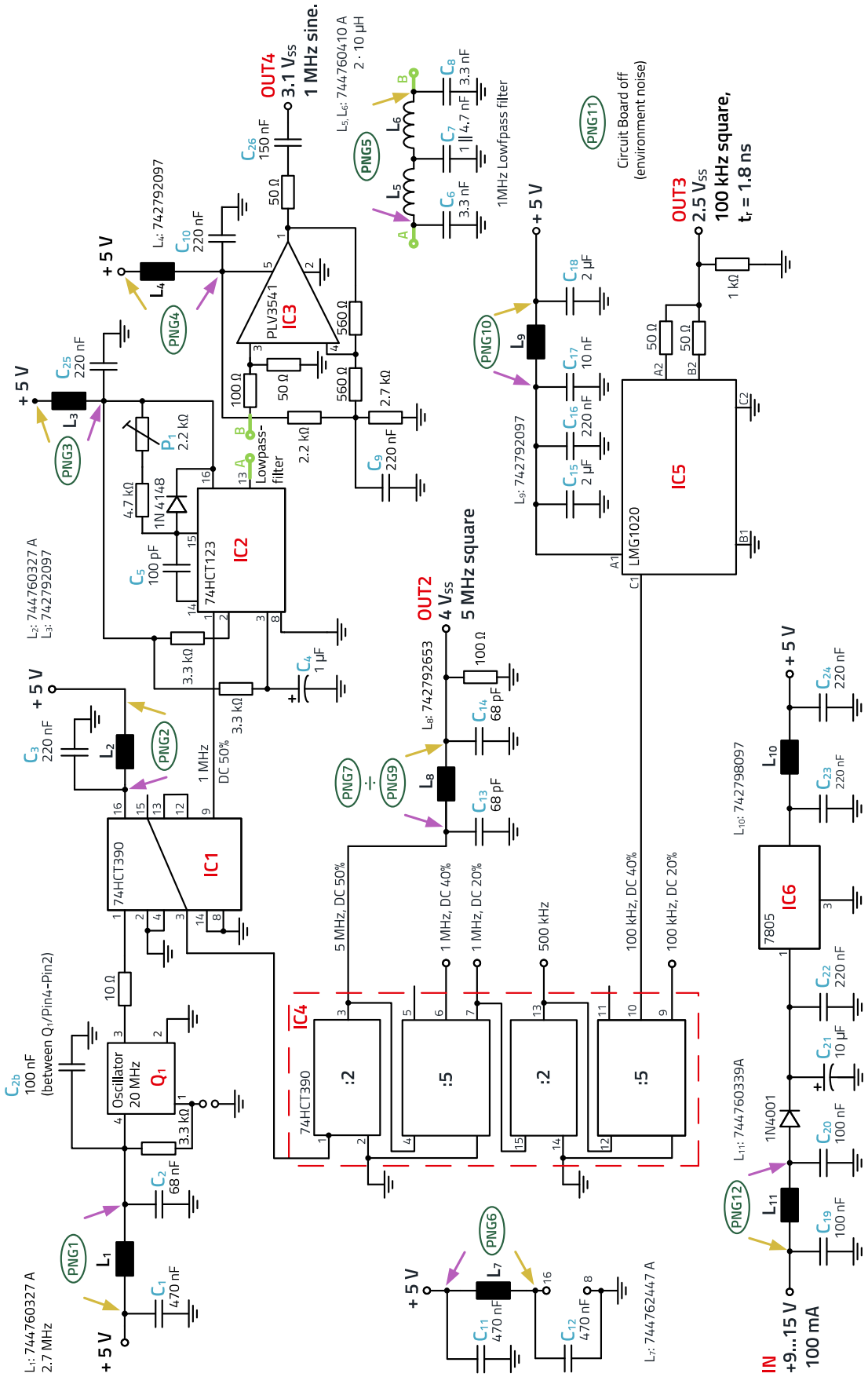

Figure 18: Circuit diagram with 'PNGxx' measuring points that are associated with the measurements of the emission from the spectrum analyzer.

PNG3:

The 1 MHz signal from IC1 only has a duty cycle (DC) of 20%. It is hard to generate a 'clean' sine-wave signal from this signal. The monoflop IC2 therefore extends the short positive signal of the 1 MHz square wave from 200 ns to 500 ns (Figure 19).

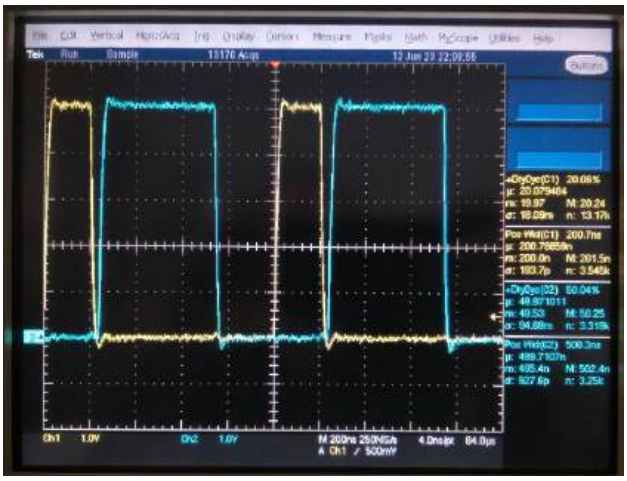

Figure 19: Extension of the 200 ns pulse with monoflop to 500 ns.

By extending the pulse to 500 ns, the output signal now has a duty cycle of 50%, i.e., the period duration is exactly 1 µs, corresponding to the 1 MHz signal. The trim pot P1 can be used to adjust the switch-on time to exactly 500 ns.

About EMC: Symmetrization to a square-wave signal theoretically eliminates the even harmonics in the frequency spectrum, leaving only the odd harmonics. In practice, the even harmonics are approx. 20 – 30 dB below the level of the odd harmonics, which contributes significantly to 'shaping' a clean sine-wave signal. Because of the different duty cycles and the switching load on the filter (low-pass filter with capacitor load C_6), the circuit generates a high interference voltage in the frequency range between approx. 10 MHz and 250 MHz. To attenuate this spectrum at IC2, the WE - CBF SMT ferrite 742792097 was selected as inductor L_3. This broadband ferrite has an impedance above 500 Ω in the relevant frequency range. The resistive part of the impedance is very high – see data sheet – which means that with the appropriate filter capacitors, high interference signal attenuation can be expected. The circuit diagram extract with the signal spectra is shown in Figure 20.

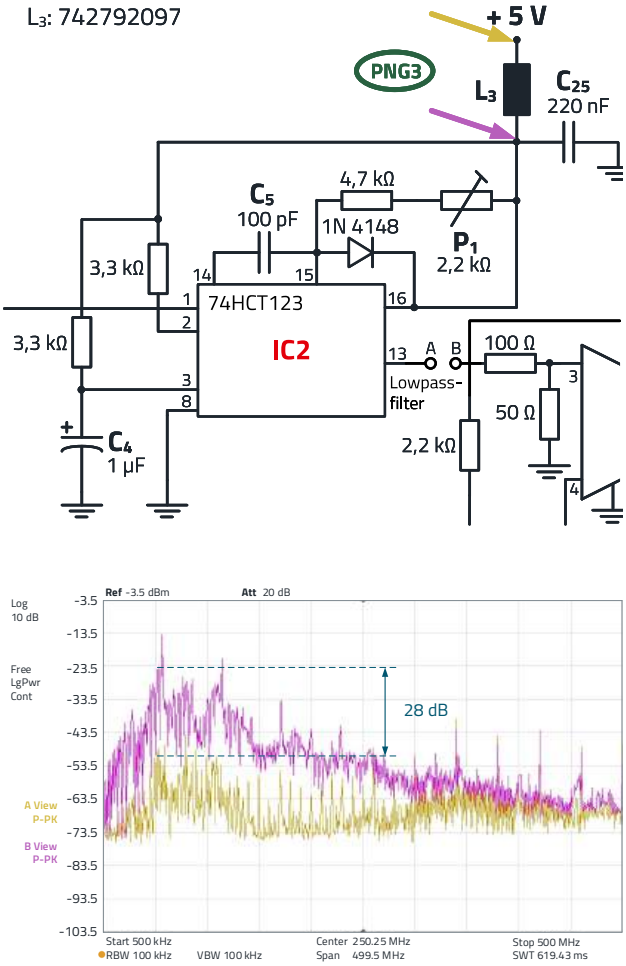

Figure 20: PNG3: V_{cc} – decoupling at monoflop IC2 with the associated interference spectra. Purple: before the ferrite, Yellow: after the ferrite.

PNG4:

IC3 (output buffer) is the impedance converter downstream of the low-pass filter. The converter essentially amplifies and buffers the 1 MHz square-wave signal smoothed by the 5th order filter into a 1 MHz sine-wave signal.

The selected operational amplifier TLV3541 has a unity gain bandwidth of 200 MHz; the amplification factor of 2 in the circuit reduces the bandwidth to 100 MHz. 'Residuals' of the harmonics that could not be sufficiently attenuated by the filter are also amplified with the signal, which is slightly noticeable in the spectrum (Figure 11).

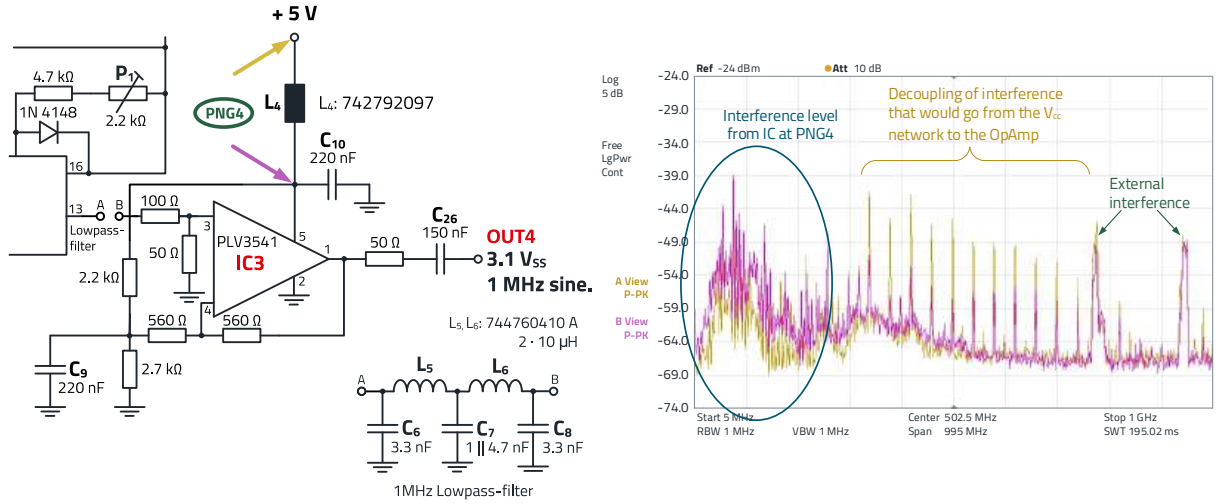

Figure 21: PNG4: V_{cc} – decoupling at OpAmp IC3 with the associated interference spectra.

However, an important aspect of the analog signal components is the attenuation of interference from the supply voltage, as decoupling of the IC from the output signal is usually not high. The problem can be seen in Figure 21. In the frequency range up to 150 MHz, the interference spectrum directly at the supply pin of the op amp dominates. Above this, the interference spectrum 'upstream' of L_4, i.e., at the supply voltage, is higher.

The interference is reduced by the IC3 filter.

It is also interesting to compare the input signal (the signal on the V_{cc} pin of IC3) with the output signal.

Figure 22 shows that the emission spectrum at the output of the op amp is approx. 3 - 5 dB lower. This means that the attenuation of the op amp is low and essentially depends on the parasitic capacitance of the load at the output.

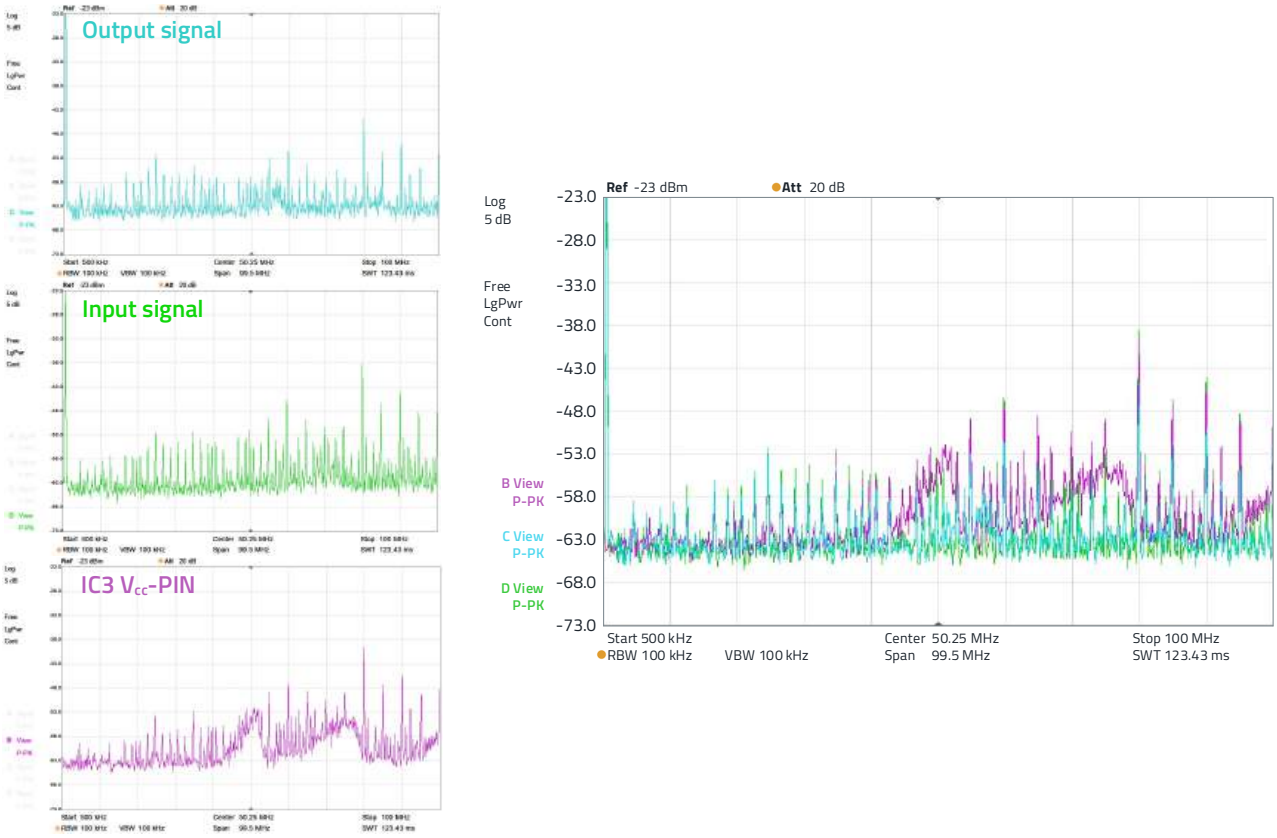

Figure 22: Emission spectra of output signal, input signal and the IC3-V_{cc} pin.

PNG6:

The frequency divider IC4 divides the 10 MHz signal down to 5 MHz and 100 kHz. The functionality of the 74HCT390 module is described in section PNG2. Here, too, PNG6 shows a very broad and dense interference spectrum (Figure 23) in the frequency range up to 500 MHz.

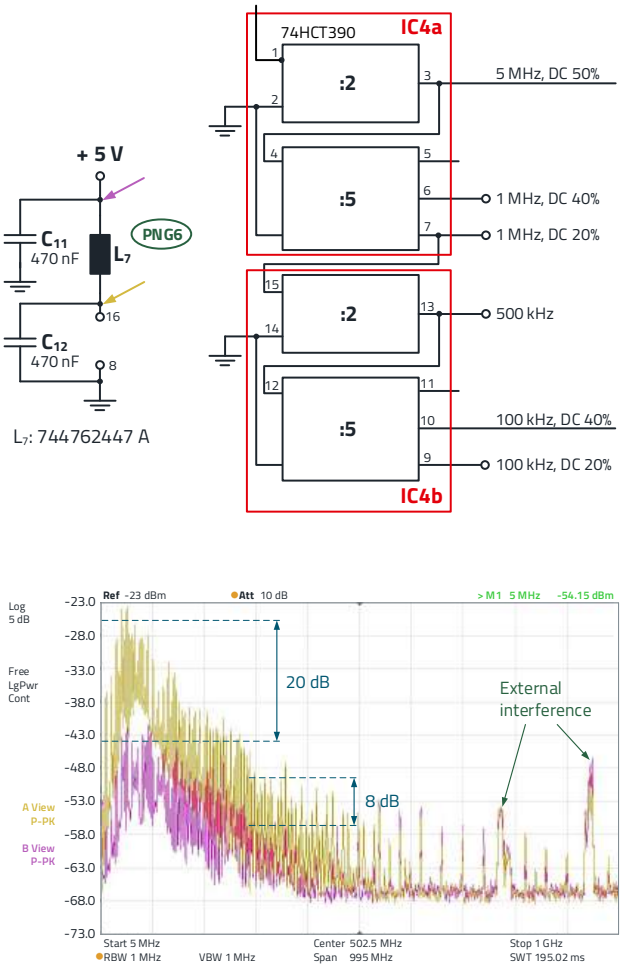

Figure 23: PNG6: V_{cc} – Decoupling at $IC4_a$/$IC4_b$ frequency divider with the associated interference spectra. Purple: after the inductor, Yellow: before the inductor.

The inductor selected was WE - RFI 744762447A. The component has an inductance of 47 µH and an impedance of > 600 Ω in the frequency range between 2 and 500 MHz.

Due to the high inductance, the reactance part of the impedance is high, but the resistive part and the high capacitance values effectively prevent resonance effects.

PNG10:

The output driver for the 100 kHz signal is described in the section 4.1. The driver is mounted on a separate circuit board with decoupling directly on the chip (1.2 mm × 0.8 mm). The WE - CBF SMT ferrite 742792097 was used for decoupling toward the power supply (see "PNG3"). MLCC capacitors in X7R and NP0 ceramic are used for decoupling directly on the chip. Figure 24 shows the circuit diagram extract and the associated interference spectra.

Decoupling of the interference spectrum is highly effective up to approx. 100 MHz, above which the capacitive and inductive coupling in the immediate vicinity of the component predominate as a result of the steep-edged switching operations. By comparison, the spectrum of the output signal shown in Figure 24 on the right is approx. 35 - 40 dB higher up to the frequency range at approx. 500 MHz.

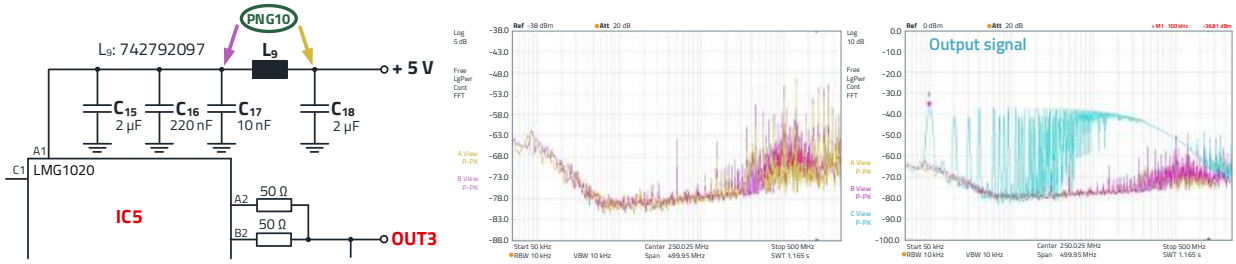

Figure 24: PNG10: V_{cc} – decoupling at the signal driver IC5 with the associated interference spectra. The light blue spectrum on the right of the image shows the output signal at 50 Ω (log. representation).

PNG12:

At the power supply input, the π filter around L_{11} is used to decouple or attenuate the interference spectrum of the entire circuit to the power supply connection. Figure 25 shows the circuit diagram extract with the associated interference spectra.

The graph shows that the attenuation over the entire frequency range from approx. 50 MHz to 1 GHz is 2 - 5 dB. The attenuation of a filter to a cable is generally far lower than in the circuit, as the insertion loss of the filter is low as a result of the high base impedance of the cable. If a higher insertion loss is required, a multi-stage filter is necessary.

.

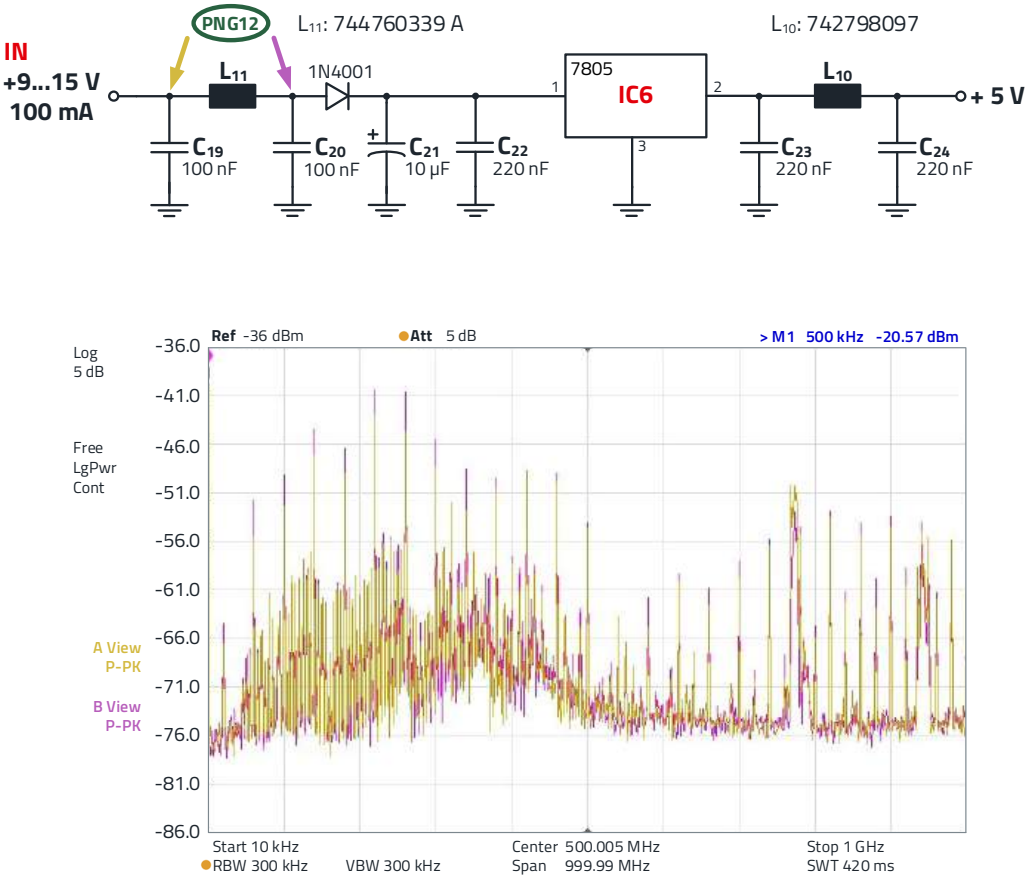

Figure 25: PNG12: V_{cc} – decoupling at the power supply input.

5. SUMMARY

Figure 26 shows the hardware set-up. The circuit was not built on a 'professional' 4-layer PCB, but purposefully on a breadboard in order to have degrees of freedom in the set-up and to clearly show the functionality of the inductors. Of course, SMT components and the layer structure can further reduce interference, but that was not the objective here. The results show how the components 'ceramic inductor', 'SMT ferrite' and 'wire-wound ferrite inductor' differ and how they can be used in the best possible way to exploit their strengths.

Overview of inductors and their most important parameters

In Table 1 there follows an overview to compare the preferred applications of the three inductors and their most important parameters.

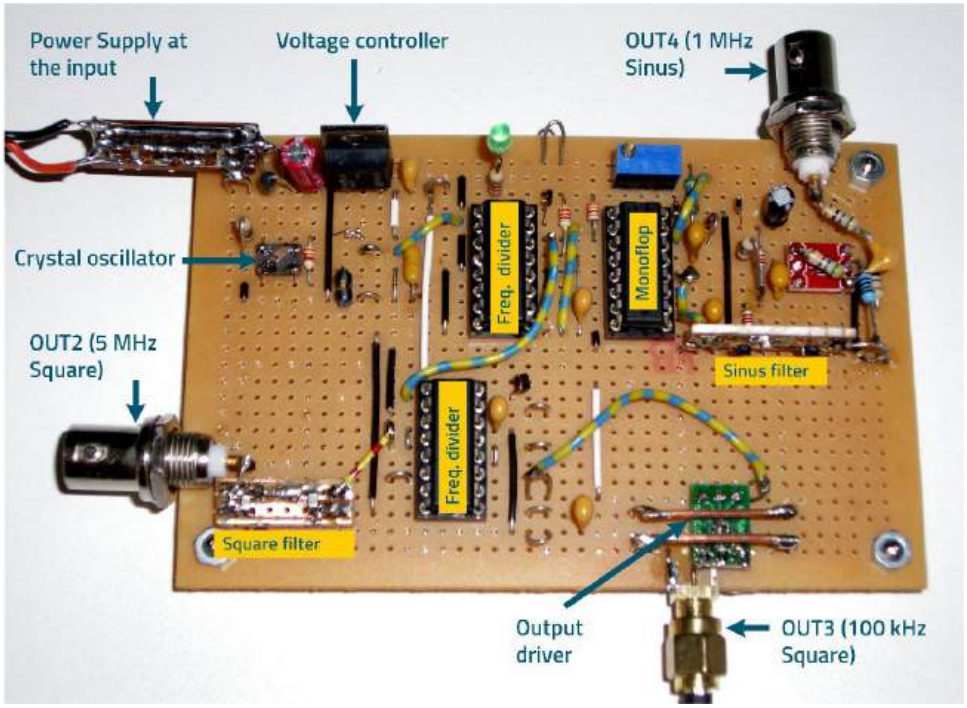

Figure 26: Hardware lab set-up for the signal generator.

Parameter	SMT ferrite	Ceramic inductor	Wire-wound ferrite inductor
Inductance range	---	low	high
Impedance range	high	low	high
Tolerance of the inductor	high	very low	low
Rated current range	high	very high	low
Loss resistance R_{DC}	low	very low	medium/high
Self-resonance frequency	high	very high	low/medium
Shape of the resonant frequency (bandwidth)	wide	narrow	narrow, multiple
Quality Q in the range below the resonant frequency	low	very high	medium
Preferred application	Attenuation/reduction of HF currents	HF filters and resonant circuits	High-frequency decoupling, steep filters, attenuation/reduction of HF currents

Table 1: Overview, comparison of the most important parameters of SMT ferrite, ceramic inductor and wire-wound ferrite inductor

A APPENDIX

A.1 References

[1] Tektronix, 75W-28152-1, 2015, Capacitance and Inductance Measurements Using an Oscilloscope and a Function Generator

[2] Texas instruments, LMG1020, SNOSD45B – FEBRUARY 2018 – REVISED OCTOBER 2018

[3] Texas instruments, TLV354x, SBOS756 – OCTOBER 2016

[4] RF Circuit Design, Joseph J. Carr, TAB Electronics 2001, ISBN 978-0071370677

[5] High-Speed Digital Design, Howard W. Johnson, Prentice Hall PTR, Englewood Cliffs, New Jersey, 1993, ISBN 0-13-395724-1

[6] Trilogie der Induktiven Bauelemente [Trilogy of inductive components], Swiridoff Verlag, Würth Elektronik, 2020, Brander, Gerfer, Rall, Zenkner, ISBN 389929151